Invest New Drugs (2008) 26:319–330
DOI 10.1007/s10637-007-9102-3

PRECLINICAL STUDIES

Murine leukemia P388 vinorelbine-resistant cell lines are sensitive to vinflunine

Ashish Aggarwal · Anna Kruczynski · Anthony Frankfurter · John J. Correia · Sharon Lobert

Received: 8 September 2007 / Accepted: 15 November 2007 / Published online: 11 December 2007

Summary The work presented here was initiated to explore the mechanisms underlying vinorelbine resistance in two previously established murine leukemia P388 cell lines (N.63 and N2.5). IC_{50} measurements demonstrated that the vinorelbine-resistant cell line N.63 was sensitive to both vinblastine and vinflunine. In addition, vinorelbine-resistant cell line N2.5 retained sensitivity to vinflunine. We used flow cytometry with propidium iodide to measure G2/M arrest in response to drug treatment. Annexin V labeling was used as a marker of apoptosis and JC-1 dye labeling as a marker of mitochondrial membrane depolarization to explore differential responses that might help explain the absence of cross resistance to vinflunine. At equipotent (10X IC_{50}) doses, after 8 h of drug treatment, vinflunine induced G2/M arrest in a significantly larger fraction of vinorelbine-resistant cells compared to vinorelbine. At the same drug doses, at 16 h after initiation of drug treatment, vinflunine induced a statistically significant greater apoptotic response and mitochondrial depolarization. The mitochondrial depolarization at 16 h was confirmed by Western blotting that showed release of cytochrome *c*. Comparison of apoptotic and mitochondrial depolarization responses in vinorelbine-resistant cells upon exposure to vinorelbine, vinblastine and vinflunine demonstrated the following pattern of drug activity: vinflunine > vinblastine > vinorelbine, confirming the importance of a antimitotic-induced mitochondria-mediated pathways in these P388 cell lines. We conclude that vinflunine may be preferred for treatment of specific cancers compared to other vinca alkaloids due to its enhanced effects on apoptotic pathways that follow G2/M arrest.

Keywords Tubulin · Tubulin isotypes · Vinflunine · Vinca alkaloids · G2/M arrest · Apoptosis · Vinca alkaloid resistance

Abbreviations

VLB	vinblastine
VRB	vinorelbine
VFL	vinflunine
MDR	Multi Drug Resistance
FITC	fluorescein isothiocyanate
PI	propidium iodide
Pgp	p-glycoprotein
FACS	fluorescence activated cell sorting
MAP	microtubule associated protein
OP-18	oncoprotein-18
qRT-PCR	quantitative real-time polymerase chain reaction

Introduction

The antimitotic agents, vinca alkaloids, constitute a major class of cancer chemotherapeutic drugs. Vincristine, vin-

A. Aggarwal · J. J. Correia · S. Lobert
Department of Biochemistry,
The University of Mississippi Medical Center,
2500 North State Street,
Jackson, MS 39216, USA

S. Lobert (✉)
School of Nursing, The University of Mississippi Medical Center,
2500 North State Street,
Jackson, MS 39216, USA
e-mail: slobert@SON.umsmed.edu

A. Kruczynski
Institut de Recherche Pierre Fabre,
81190 Castres, France

A. Frankfurter
Department of Biology, University of Virginia,
Charlottesville, VA, USA

blastine, and vinorelbine are widely used in combination chemotherapy for both solid and hematological tumors. Since the arrival of naturally occurring vinca alkaloids like vinblastine and vincristine [29], additional semi-synthetic vinca alkaloids have been introduced with the help of medicinal chemistry. Vinflunine (20′, 20′-difluoro-3′, 4′-dihydrovinorelbine), is the most recent addition to this family of compounds and is uniquely synthesized from a vinca precursor compound with the addition of two fluorine atoms which have been shown to improve the therapeutic index as compared to the non-fluorinated compound [13, 15, 17]. Vinflunine is currently in Phase III studies for transitional cell carcinoma of the urothelium, non-small cell lung cancer and metastatic breast cancer. Vinca alkaloids bind at the interdimer interface of the α and β tubulin subunits with different affinities [11, 20] and their therapeutic doses are inversely proportional to their overall binding affinities [24]. All vinca alkaloids suppress microtubule dynamics and induce G2/M arrest and apoptosis; although in some cells this occurs only at high doses [30]. Vinflunine is the least potent of the clinically useful vinca alkaloids [16, 22, 23] however, it has improved efficacy for some tumors relative to other vinca alkaloids [13]. While the mechanism(s) by which vinca alkaloids induce apoptosis after mitotic arrest are not well established, the earliest sign of apoptosis following treatment with another antimitotic agent, docetaxel, is the collapse of the mitochondrial potential following G2/M arrest [10]. Kruczynski et al. [18] demonstrated that vinflunine causes caspase-3/7 activation and other apoptotic events such as phosphorylation of Bcl-2 in a human leukemia cell line and PARP degradation and DNA fragmentation in P388 cells. More detailed studies comparing vinflunine with other vinca alkaloids are required to understand the differential efficacy.

Resistance to chemotherapy can occur initially or after repeated treatment cycles. Thus, understanding vinca alkaloid induced apoptotic pathways and tumor resistance mechanisms are critical for improving therapies; although it is likely that several factors may contribute to the antimitotic drug resistance that occurs in certain cells [7]. Over-expression and activity of the P-glycoprotein (Pgp) efflux pump, a 170 kDa energy dependent membrane glycoprotein, is the major reason for multiple drug resistance in many tumor cells [4]. However, differential responses within one class of drugs, such as the vinca alkaloids, can not be explained by Pgp alone. Changes in relative amounts of specific β-tubulin isotypes that alter the assembly state of microtubules may contribute to resistance to antimitotic agents (i.e. vinca alkaloids or taxanes) [1, 2, 12, 27]. Although, since vinca alkaloids bind with the same affinity to purified tubulin isotypes, differential binding to tubulin isotypes is not likely to explain differential cell responses to vinca alkaloids [22].

In an attempt to understand the differential cell responses of vinca alkaloids, we compared the effects of high dose (10X IC_{50}) vinblastine, vinorelbine and vinflunine in vinorelbine-sensitive and -resistant cell on events leading to leukemia cell death: G2/M arrest, mitochondrial depolarization, apoptosis, and cytochrome *c* release from mitochondria in vinorelbine-sensitive and -resistant murine P388 cells. Vinorelbine-resistant cells were shown to retain sensitivity to vinflunine. We found no significant differences in microtubule fractions, total tubulin or β-tubulin isotype levels in vinorelbine-sensitive and -resistant cells, ruling out a simple tubulin-based mechanism of drug response. Vinflunine induced apoptosis in a significantly larger fraction of cells compared to vinorelbine in all cell lines studied. This was associated with depolarized mitochondrial membranes, cytochrome *c* release and a larger fraction of cells in G2/M arrest.

Materials and methods

Cell culture

Two vinorelbine-resistant P388 mouse leukemia cell lines were developed as described previously [9]. Parental and resistant cells were grown in RPMI-1640 media (ATCC, Manassas, VA) supplemented with 10% horse serum and 20 μM β-mercaptoethanol in the presence antibiotic/antimycotics. All experiments were done within first 12 passages and cells were not grown more than 3 weeks continuously.

IC_{50} studies by trypan blue exclusion method

The antiproliferative effects of vinca alkaloids on P388 vinorelbine-sensitive and -resistant cells were determined by measuring IC_{50} values which represent the concentration of a drug that is required for 50% inhibition of cell proliferation. The IC_{50} values for each cell line were measured five times by trypan blue exclusion method over time period of 2 years. In these experiments, 10^4 cells/ml per well were seeded in 24 well plates and were allowed to grow overnight to reach log growth phase. They were then treated with 11 serial dilutions (ranging approximately 2 log units above and below the IC_{50} of the drug) in duplicate wells. Water replaced drug in duplicate control wells. After a 48 h incubation with drug, 100 μl of trypan blue reagent (Cambrex Bioscience, Walkersville, MD) were added to each well and the cells were passed through a syringe and needle (BD eclipse 1 ml syringe and 27G 0.4×13 mm needle) to break the cell aggregates and mix the dye. Cells from each well were counted using a hemocytometer. Data were plotted as the cell number versus the drug concentration and were fit by nonlinear exponential decay using

Origin® 6.0 software (Microcal Software, Inc., Northampton, MA). The IC_{50} was calculated using formula $IC_{50}=-t1*(\ln(1/2))$, where $t1$ is the relaxation time for the first order exponential decay.

P-glycoprotein functional levels by flow cytometry

The functional levels of P-glycoprotein were determined by quantitative measurement of the export of dyes ($DiOC_2$ and Rh-123), which are substrates of P-glycoprotein, using an FC 500 cytometer (Beckman Coulter, Fullerton, CA). 2×10^6 cells were centrifuged and resuspended in 2 ml pre-warmed RPMI-1640 media without supplements. The cell suspension was then divided equally in two 12×75 mm polystyrene tubes (BD Labware, Franklin Lakes, NJ). Both samples were incubated with 5 μM Rh123 dye in the absence or presence of 100 μM verapamil. The verapamil containing tube served as a negative control since verapamil is an inhibitor of P-glycoprotein. The dye influx into the cells was allowed for 10 min in 5% CO_2 incubator at 37°C. After centrifugation at 50×*g* for 5 min, the cells were resuspended in fresh pre-warmed RPMI-1640 media. Again 100 μM verapamil were added to block P-glycoprotein in the control tube. Efflux was then allowed for 10 min in a CO_2 incubator. After incubation, cells were immediately centrifuged at 50×*g* for 5 min and resuspended in cold 0.5 ml RPMI-1640 media. This was followed by FACS analysis. The same procedure was used to assess the efflux of $DiOC_2$ dye (10 μg/ml final concentration).

β-Tubulin isotype protein levels by quantitative western blotting

We developed a quantitative Western blotting technique that is highly reproducible and sensitive and have previously reported our methods [14]. We used monoclonal antibodies: SAP4G5 (Sigma Aldrich, St. Louis, MO) for β-tubulin class I, 7B9 for β-tubulin class II, TUJ1 for β-tubulin class III and 10A2 for β-tubulin class IV. The reactivity and specificity of SAP4G5, 7B9 and TUJ1, 10A2 have been previously described [14, 19, 21, 22, 31].

Total tubulin content by western blotting

The total tubulin contents of P388 vinorelbine-sensitive and -resistant cell lines were compared by quantitative Western blotting. The pan-β-tubulin antibody Tu27 [5] was used in the same procedure for Western blotting described in the previous section. An antibody raised against Glyceraldehyde 3-phosphate dehydrogenase (GAPDH) was used to verify relatively equal loading of total protein and to normalize total tubulin (anti-GAPDH antibody, 6C5, Chemicon, Temecula, CA).

Free tubulin and polymerized microtubule fractions by western blotting

Free and polymerized tubulin fractions from cell lysates were prepared using two different buffers: Buffer 1 (2 M glycerol, 100 mM Tris HCl, pH 6.8, 0.5% Nonidet P-40, 1 mM $MgCl_2$, 2 mM EGTA) or Buffer 2 (4 μg/ml taxol, 20 mM Tris HCl, pH 6.8, 0.14 M NaCl, 0.5% Nonidet P-40, 1 mM $MgCl_2$, 2 mM EGTA) [27]. We added Complete® protease inhibitor cocktail (Roche Applied Science, Indianapolis, IN) to minimize proteolysis of the samples. Cells were suspended in 500 μl of buffer and lysed using a manual dounce cell homogenizer either on ice for the taxol buffer or in 37°C water bath for the glycerol buffer. After complete lysis of the cells, which was confirmed under a microscope by the loss of intact plasma membranes, lysates were centrifuged at 12,000×*g* for 10 min at 4°C for the taxol buffer or at 350,000×*g* for 5 min at 37°C for the glycerol buffer. Supernatants which contained the free tubulin fraction were collected carefully. SDS sample buffer was added to both the supernatant and pellet fractions, mixed and boiled for 2 min. We estimated the percentage of free tubulin in the supernatants and polymerized tubulin in the pellets by quantitative Western blotting using pan-β-tubulin antibody, Tu27. Duplicate Western blots were carried out on three biological preps.

G2/M arrest by propidium iodide staining and flow cytometry

G2/M arrest was assessed by propidium iodide (PI) staining and flow cytometry. 2.5×10^5 cells/well were grown overnight in 12 well plates. When they reached log phase of growth; vinblastine, vinorelbine or vinflunine was added at 10X IC_{50} values for P388-S. 10X IC_{50} concentrations were chosen to assure G2/M arrest. We did not observe significant G2/M arrest in when cells were treated with the IC_{50} drug concentration. After 4, 8, 16, 24 and 48 h of incubation with 5% CO_2 at 37°C, the cells were centrifuged and resuspended in 0.5 ml ice cold PBS in 12×75 mm polystyrene tubes. The samples were each mixed with 3.5 ml of ice cold 70% ethanol, vortexed and incubated for at least 2 h at −20°C in order to fix the cells. The cells were then centrifuged at 450×*g* and the pellet was washed with 4 ml ice cold PBS, centrifuged and resuspended in 0.5 ml ice cold PBS containing 20 μg/ml PI. After a 30 min incubation in the dark at 4°C, the cells were washed twice with ice cold PBS and resuspended in 0.5 ml PBS. FACS analysis was done using a FC 500 cytometer (Bechman Coulter, Fullerton, CA) and data were analyzed using FCS Express Software (De Novo Software, Ontario, Canada). Two independent experiments were carried out for each sample.

Apoptosis assay by AnnexinV-FITC/PI dual labeling and flow cytometry

Early apoptosis was assessed by dual labeling of cells with Annexin-FITC and PI followed by flow cytometry. 2.5×10^5 cells/well were grown overnight in 12 well plates. When the cells reached log phase of growth, vinblastine, vinorelbine or vinflunine was added at 10X IC_{50} values for P388-S. After 4, 8, 16, 24, 48 h, the cells were harvested and centrifuged at 100×*g* for 5 min and resuspended in 1 ml cold binding buffer (10 mM Hepes/NaOH (pH 7.4), 140 mM NaCl, 2.5 mM $CaCl_2$). One hundred microliters of this suspension were transferred to 12×75 mm polystyrene tube. Five microliters of AnnexinV-FITC reagent (BD Pharmingen, San Jose, CA) and 40 µl of 200 µg/ml PI stock were added and mixed. The samples were then incubated for 30 min to 1 h on a shaker in the dark at room temperature. Three hundred-fifty microliters of cold binding buffer were added before analysis by FACS. Data were analyzed using FCS Express Software and the percentage of live cells was plotted against the drug treatment time in hours. Two independent experiments were done for each condition.

Mitochondrial membrane potential change by JC-1 dye using flow cytometry

Mitochondrial membrane potential was assessed by Mito-GLO kit (Imgenex, San Diego, CA) according to the instructions supplied with the kit. Cells of 2.5×10^5 per well were grown in 12-well culture plates overnight. When the cells were at log growth phase vinblastine, vinorelbine or vinflunine was added at the 10X IC_{50} concentrations of P388-S. After 2, 3, 4, 8, 16 and 24 h, cells were harvested, centrifuged at 400×*g* for 5 min at room temperature and incubated with 0.5 ml pre-warmed MitoGLO working solution containing the JC-1 Dye (5,5′,6,6′-tetrachloro-1,1′,3,3′-tetraethylbenzimidazolcarbocyanine Iodide) and 40 µM progesterone to block Pgp mediated export. The cells were gently vortexed to break any clumping and incubated for 15 min at 5% CO_2 and 37°C. After the incubation period, the cells were washed twice with the working buffer containing progesterone, centrifuged at 400×*g* for 5 min and finally resuspended in 0.5 ml working buffer containing progesterone prior to FACS. Red JC-1 oligomers, which were rich in live cells with polarized mitochondria, were gated in the FL1 Channel and green JC-1 monomers, which were rich in early apoptotic cells with depolarized mitochondria, were visualized under the FL3 Channel using FCS Express Software. The fold-increase in cells containing depolarized mitochondria compared to the control was plotted against drug treatment time in hours. Two to four independent experiments were done for each condition.

Cytosolic cytochrome *c* levels by western blotting

Cells were grown to confluence for 24 h and then they were exposed to 10 X concentration of P388-S IC_{50}. For vinblastine, vinorelbine or vinflunine, the cells were harvested after 0 and 16 h and cytosolic and mitochondrial fractions were prepared using the Cytochrome *c* Release Apoptosis Kit (Calbiochem, San Diego, CA). Briefly, 5×10^7 cells were collected by centrifugation at 600×*g* at 4°C and then washed with 10 ml cold PBS. After centrifugation at 600×*g* at 4°C, the cells were resuspended in the cytosol extraction buffer mix and incubated on ice for 10 min. The cells were then lysed with the manual dounce homogenizer. Lysis of cells was confirmed by loss of intact plasma membranes of approximately 80–90% cells visually under the microscope. The cell lysate was centrifuged at 700×*g* for 10 min at 4°C. The supernatant was transferred to a new tube and again centrifuged at 10,000×*g* for 30 min at 4°C to separate the cytosolic and mitochondrial fractions. The supernatant containing the cytosolic fraction was transferred to a separate tube. The mitochondrial pellet was suspended in the mitochondrial buffer (supplied with the kit), mixed and vortexed for 15 s. The protein concentrations were determined using Advanced Protein Assay Reagent (Cytoskeleton Inc., Denver, CO) and were adjusted to 10 µg/µl using SDS sample buffer, mixed and boiled for 10 min. Proteins were resolved on a 15% SDS-polyacrylamide gels to visualize cytochrome *c* using anti-cytochrome *c* antibody (BD Pharmingen, San Jose, CA).

Results

Characterization of vinorelbine-resistant P388 cell lines

IC_{50} measurements

The IC_{50} values for the P388-S, P388-N.63 and P388-N2.5 cells ranged from 0.6 nM to near 22 nM for the three drugs

Table 1 IC_{50} values of vinca alkaloids for P388 vinorelbine-sensitive and -resistant cell lines

Drug	Cell line	IC_{50} (nM)	S.D.	Fold resistance
Vinblastine	P388-S	0.6	0.2	
	P388-N.63	1.1	0.2	2
	P388-N2.5	4.0	1.2	7
Vinorelbine	P388-S	1.0	0.1	
	P388-N.63	16.0	2.1	17
	P388-N2.5	8.3	0.4	9
Vinflunine	P388-S	11.1	4.0	
	P388-N.63	12.1	4.0	1
	P388-N2.5	21.9	10.8	2

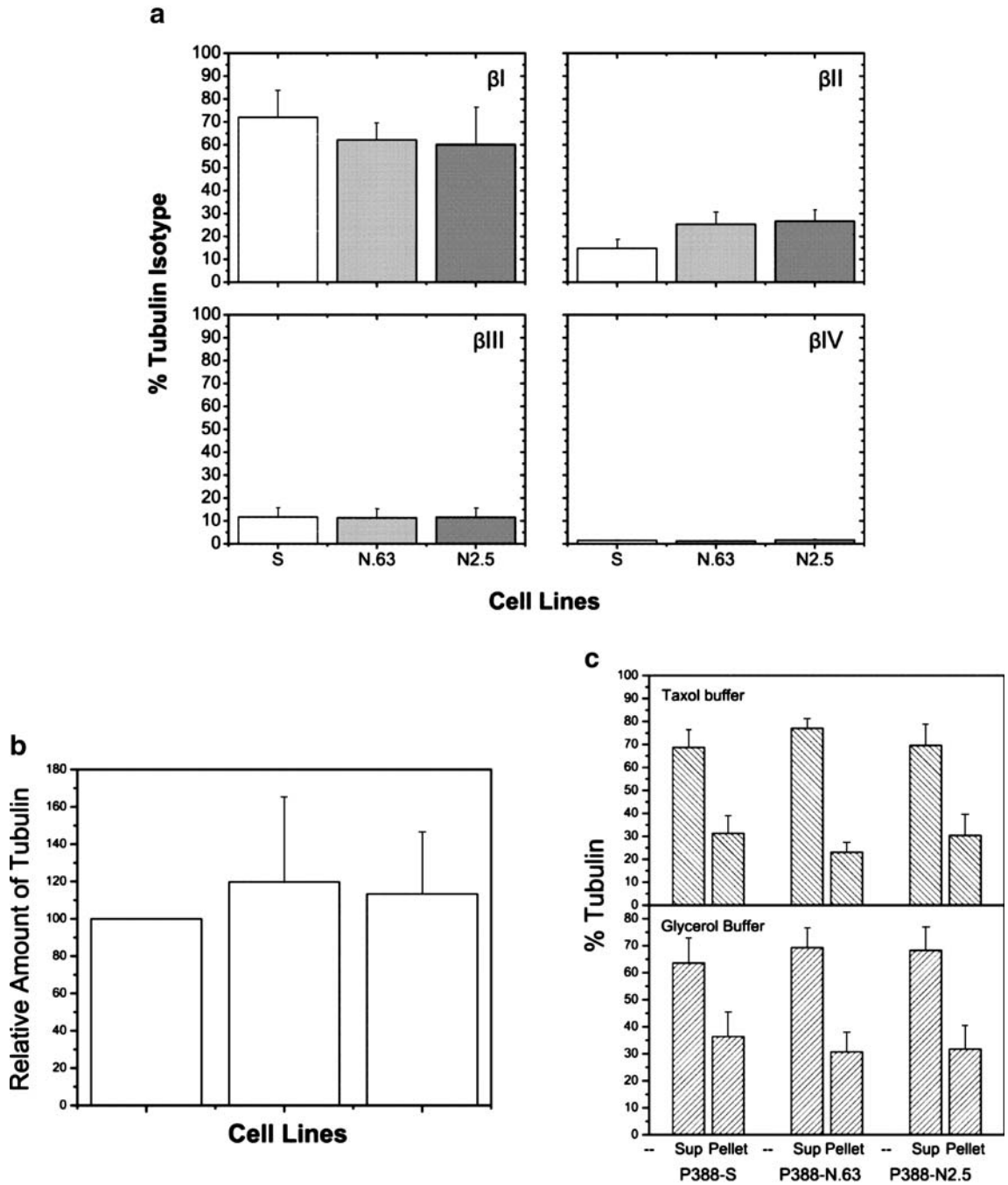

Fig. 1 Distribution of β-tubulin isotypes, total tubulin content and polymerized microtubule fraction in P388 vinorelbine-sensitive and -resistant cell lines by Western blotting. **a** Monoclonal antibodies to β-tubulin isotypes I, II, III and IVa + IVb were used to measure the percentage of each β-tubulin isotype in these cell lines by Western blotting. The sum of these isotypes was considered to be the total tubulin for analysis. Each error bar represents the standard deviation from biological and technical triplicates. **b** Anti β-tubulin antibody Tu27 was used to compare total tubulin levels by Western blotting and densitometry. Anti-GAPDH antibody was used to determine GAPDH levels in cell lysates as a loading control. Tubulin densities were normalized to GAPDH densities. The value for P388-S cells was set to 100. Each error bar represents the propagated error from three independent experiments. **c** Cells were lysed in the presence of Taxol or Glycerol buffer. Microtubule polymers were found in the centrifuged pellets; whereas free tubulin was retained in supernatant. Each bar represents the fraction of free tubulin or polymerized tubulin. The error bars show the propagated standard deviations from three preps and at least two sets of experiments for each prep

studied (vinblastine, vinorelbine and vinflunine) (Table 1). The results are consistent with data reported for L1210 leukemia cells where the IC_{50} values were ranked by potency: vinblastine > vinorelbine > vinflunine. The vinorelbine IC_{50} values for P388-N2.5 and N.63 cells were 9 and 17 times higher than for P388 S cells. The values for vinblastine were 7 and 2 times higher than for the parental cell line. However, these cells were still relatively sensitive to vinflunine, with IC_{50} values the same as or only two-fold higher than the control cells.

P-glycoprotein (MDR1 and MRP1)

ABC transporters play a role in the transport of drugs and drug conjugates. Their importance for the efflux of vinca alkaloids from cells has been reported [8]. Classically this role is exemplified chiefly by MDR1 (P-glycoprotein, MDR/ABCB sub-family) and MRP1 (MRP/ABCC sub-family) [3]. The Rh123 (rhodamine 123) dye is a substrate for both MDR1 and MRP1 sub-family proteins and $DiOC_2$ dye is a specific substrate for only the MDR1 sub-family [26]. We used flow cytometry to measure the efflux of Rh123 or $DiOC_2$ in the presence and absence of verapamil to determine basal levels of functional ABC transporters (MDR1 and MRP1 pumps) in P388 vinorelbine-sensitive and -resistant cell lines. Verapamil is commonly used to study ABC transporters because it is a potent blocker. Functional levels of both MRP1 and MDR1 transporters were found to be elevated in vinorelbine-resistant P388 cell lines (data not shown). While these results suggest that MDR1 and MRP1 contribute to vinca alkaloid resistance in these cell lines, they do not explain the relative sensitivity of vinorelbine-resistant cell lines to vinflunine.

β-Tubulin isotype distribution, total tubulin content, microtubule content

There are seven β-tubulin isotype classes based upon their carboxyl terminal sequences [33]. We compared β-tubulin I, II, III and IVa + IVb isotype protein levels in P388 vinorelbine-sensitive and -resistant cell lines using quantitative immunoblotting (Fig. 1a). We found that class I was the major β-tubulin isotype in all three cell lines (60–72% of total β-tubulin) while β-tubulin classes IVa + IVb were the least abundant (1.2–1.7% of total β-tubulin). β-Tubulin class III was constant in all cell lines (11.3–11.7% of total β-tubulin), and there were no significant differences in β-tubulin classes I, III and IV ($p>0.05$) among P388 vinorelbine-sensitive and -resistant cells. The only significant difference was in β-tubulin class II isotype levels ($p<0.05$) where this isotype was 25.3+5.5% of total β-tubulin in P388-N.63 and 26.6+4.8% in P388-N2.5 compared to 14.8+3.8% of total β-tubulin in P388-S. While it is unlikely that minor changes in β-tubulin class II alone can produce vinca alkaloid resistance phenotype [2], this result also does not explain the enhanced activity of vinflunine compared to vinblastine or vinorelbine in these resistant cell lines. Note while not dramatic, the upregulation of β-tubulin class II is in part compensated by a decrease in β-tubulin class I. This explains the constant total tubulin levels.

Because a variation in total tubulin content can be a cause for antimitotic resistance [35], we measured the total tubulin content in these cell lines by Western blotting. The value for P388-S cells was set to 100. We found no statistically significant difference ($p<0.05$) in total tubulin content in either P388-N.63 (119.8+45.4) or P388-N2.5 (113.2+33.3) when compared to P388-S (Fig. 1b).

Minotti et al. [27] showed that a higher microtubule polymer fraction can be associated with resistance to vinca

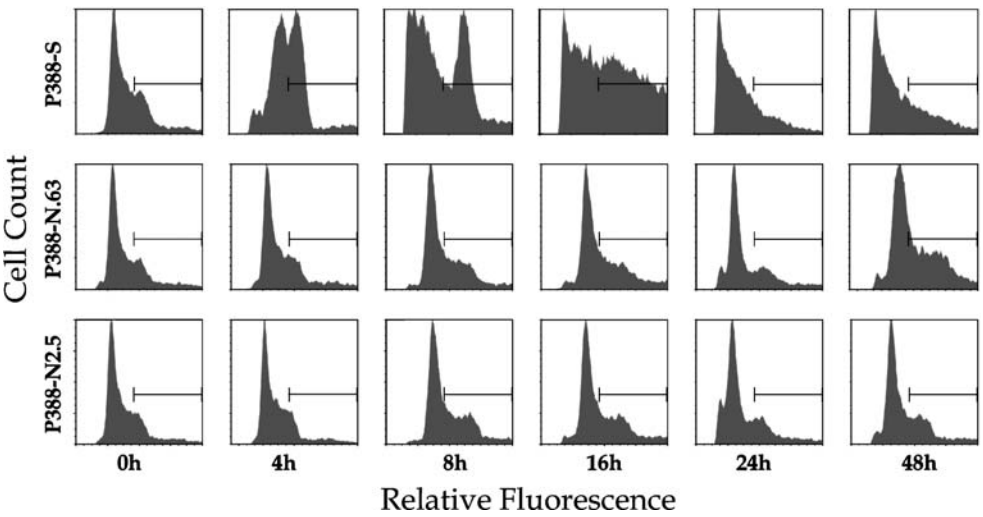

Fig. 2 G2/M arrest by vinorelbine in P388 vinorelbine-sensitive and -resistant cell lines by flow cytometry. Cells were treated with vinorelbine at 10X IC_{50} concentration for P388-S cells (10 nM vinorelbine) and for 0, 4, 8, 16, 24, 48 h. After treatment, G2/M arrest was assessed by PI staining using flow cytometry. P388-S cells show G2/M arrest at 4 and 8 h and a significant hypodiploid (apoptotic) fraction beginning at 8 h which was not found in either vinorelbine-resistant cell line. The experiments were repeated twice for each time point with independent cell preps

alkaloids. To investigate if this mechanism is responsible for vinca alkaloid resistance in our cell lines, we used quantitative Western blotting to measure the tubulin fraction in the polymerized and free forms in P388-S and vinorelbine-resistant cell lines. We used two different buffers containing either taxol or glycerol as cellular microtubule stabilizers. These buffers have been well studied for preserving cellular microtubules [27]. With the glycerol buffer, we measured 36.4+9.2% tubulin in the microtubule fraction (pellet) in P388-S compared to 30.7+7.4% in P388-N.63 and 31.7+8.7% in P388-N2.5 (Fig. 1c). Similarly, with the taxol buffer, we measured 31.3+7.6% cellular tubulin polymerized in the microtubule fraction in P388-S compared to 23.0+4.3% in P388-N.63 and 30.3+9.3% in P388-N2.5 (Fig. 3c). Analysis by Student t test demonstrated that the differences between polymerized microtubules in vinorelbine-resistant P388 cells and P388-S were not statistically significant ($p<0.05$ for all comparisons). Furthermore, a decrease in polymer levels would be consistent with sensitivity to vinca alkaloids and thus these results do not explain the mechanism of resistance.

Cell responses to vinorelbine

G2/M arrest and apoptosis

Having ruled out a tubulin- or microtubule-based mechanism of drug resistance in these cell lines, we investigated the apoptotic pathways induced by vinorelbine to establish a baseline for comparison with other vinca alkaloids. We used propidium iodide (PI) labeling and flow cytometry to measure the percentage of cells in G2/M phase after 0, 4, 8, 16, 24 and 48 h exposure to vinorelbine (10X IC_{50} for P388-S). The total percentage of cells in G2/M phase was significantly reduced in P388 vinorelbine-resistant cell lines when compared to P388-S at 4 and 8 h after treatment with vinorelbine (Fig. 2). After just 4 h, 47.5% vinorelbine treated cells were in G2/M phase in P388-S cells, whereas only 27.9% P388-N.63 cells and 21.9% P388-N2.5 cells were in G2/M phase after 4 h (Fig. 3a). At subsequent time points, there was an increase in the sub-G1 hypodiploid peak in P388-S that was not found in the resistant cells (Fig. 2).

Annexin-V is a 35 kDa protein that binds to translocated phosphatidyl-serine on the outer plasma membrane. Its binding is evidence of early stages of apoptosis. We used AnnexinV-FITC/PI dual labeling to measure the cytotoxic effects of vinorelbine by flow cytometry. Vinorelbine treatment failed to cause extensive Annexin V binding in the resistant cell lines (Fig. 3b). However, in the P388 sensitive cell line, Annexin V labeling demonstrated that more than 95% of cells were in the apoptotic and/or necrotic phase in 48 h, while only 39.5% P388-N.63 cells and 29.4% P388-N2.5 cells were in apoptotic and/or necrotic phase after 48 h.

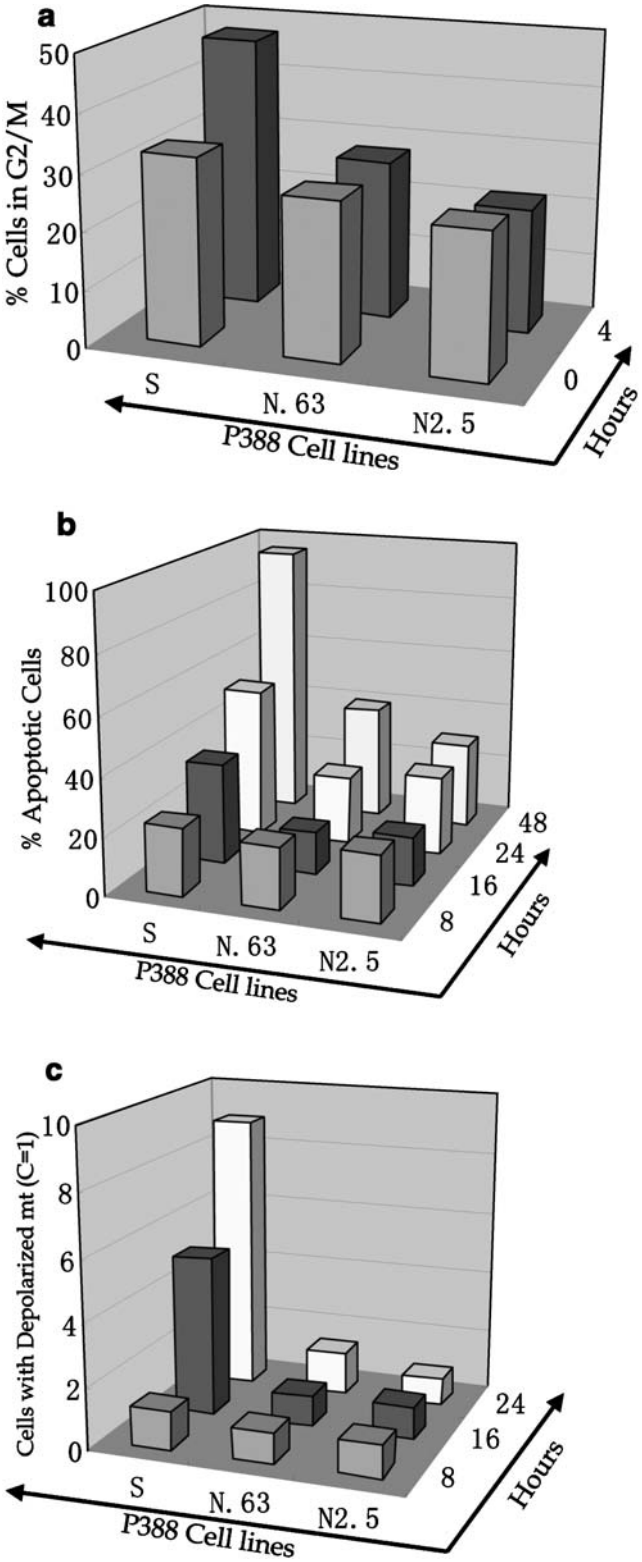

Fig. 3 Diminished effect of vinorelbine on P388 resistant cell lines. Cells were treated with 10 nM vinorelbine (10X IC_{50} for P388-S cells) for shown time points after which G2/M arrest (**a**), apoptosis (**b**), and depolarized mitochondria (**c**) were measured by flow cytometry. In the3D plots, the *X* axis represent the cell lines, the *Y* axis represent the extent of drug effect and the *Z* axis shows the time points

Disruption of the mitochondrial membrane potential is one of earliest signs of apoptosis and leads to the release of cytochrome *c* [32]. We employed the cytofluorimetric analysis of the mitochondrial membrane potential using the J-aggregate forming lipophilic cation, 5′,6,6′-tetrachloro-1,1′,3,3′-tetraethylbenzimidazolcarbocyanine iodide (JC-1) dye [6]. When P388-S cells were treated with vinorelbine for 24 h, there was a ninefold increase in cells with collapsed mitochondrial potential compared to the control (Fig. 3c). On the other hand, there was only 1.4 fold increase in cells having depolarized mitochondria in P388-N.63 and no change in P388-N2.5 after 24 h.

Cell responses to vinblastine and vinflunine

G2/M arrest

Both vinblastine and vinflunine caused extensive G2/M arrest in P388 sensitive cells after 8 h (Figs. 4 and 5). Vinblastine treatment led to 77.2+0.1% of the cells in G2/M whereas vinflunine arrested 80.6+3.1% cells after 8 h. Vinflunine's effect on P388-N.63 cells was similar to vinblastine after 8 h (47.9+0.2% and 41.6+3.36% G2/M cells respectively) (Fig. 5). In addition, vinflunine treatment resulted in significant G2/M arrest (65.6+1.3%) in P388-N2.5 cells after 8 h compared to vinblastine treatment (49.7+3.2%) (Fig. 4). After 8 h of vinflunine or vinblastine treatment the fraction of cells in the hypodiploid apoptotic peak increased in all cell lines (Fig. 4). Overall the effect of these drugs on the percentage of cells in G2/M arrest was vinflunine > vinblastine > vinorelbine.

Apoptosis

Annexin V/PI dual labeling was used to compare vinblastine and vinflunine effects on apoptosis at 10X IC_{50} P388-S concentrations. Vinflunine was highly toxic to P388-S cells as only 2.5+2.0% cells survived at 24 h and just 0.9+0.3% after 48 h (Fig. 6). Vinblastine also was highly toxic to P388-S cells with survival of only 14.1+2.4% cells after

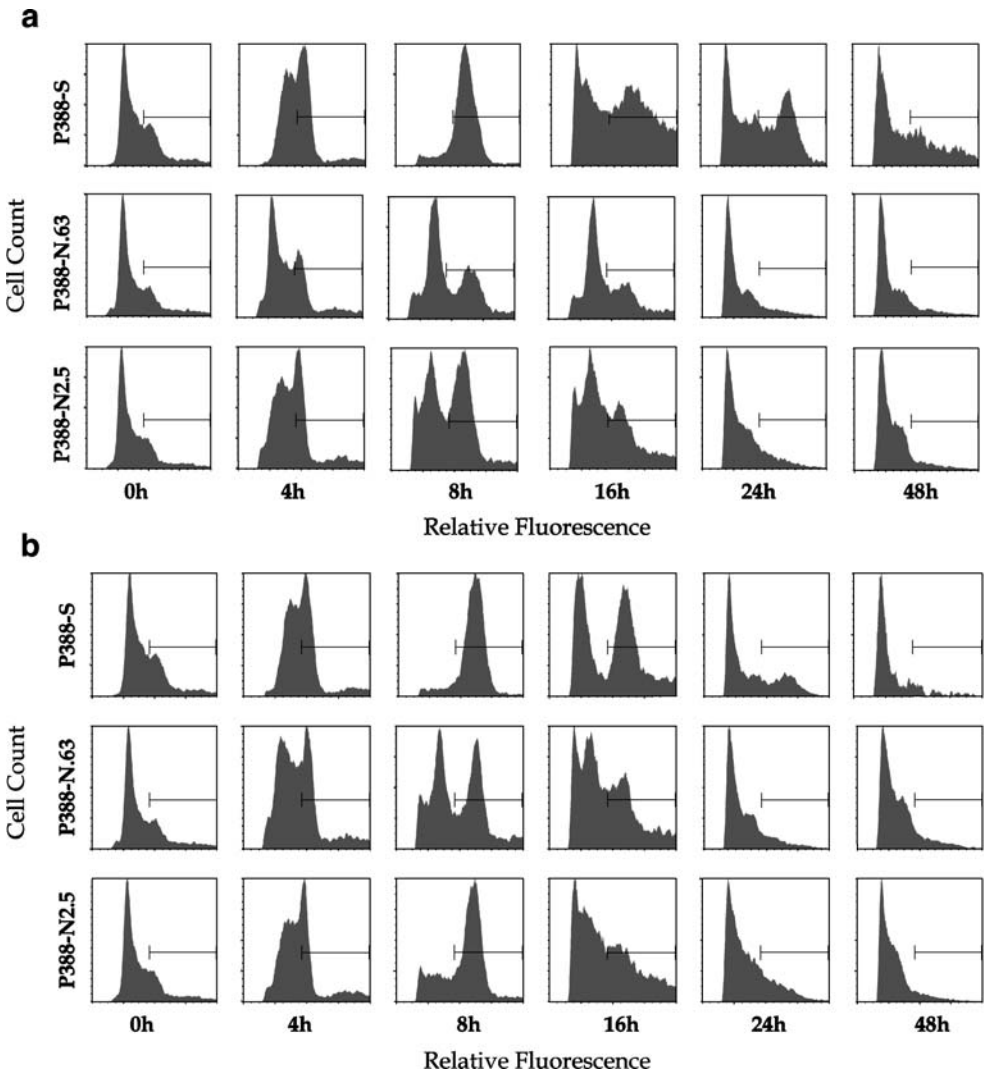

Fig. 4 G2/M arrest by vinblastine and vinflunine in P388 vinorelbine- sensitive and -resistant cell lines by flow cytometry. Cells were treated at 10X IC_{50} concentrations for P388-S cells with 6 nM vinblastine (**a**) and 110 nM vinflunine (**b**). After 0, 4, 8, 16, 24, 48 h of treatment, G2/M arrest was assessed by PI staining using flow cytometry. The P388-S cells show G2/M arrest at 8 h induced by vinblastine and vinflunine at 10X IC_{50} concentrations. The experiment was repeated twice for each time point with independent cell preps

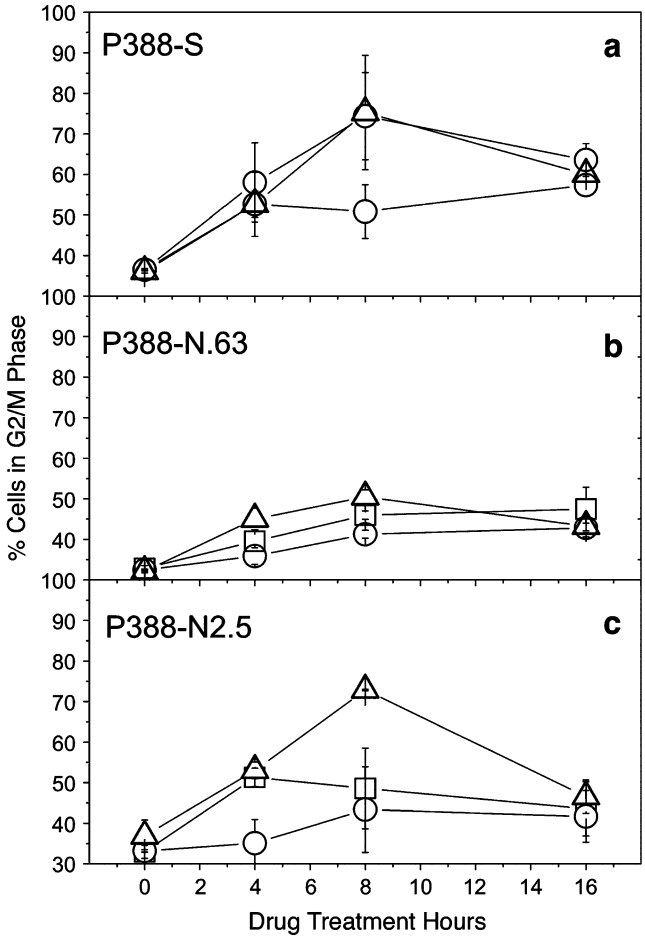

Fig. 5 G2/M arrest by vinca alkaloids in P388 vinorelbine-sensitive and -resistant cell lines by flow cytometry. Cells were treated with at 10X IC_{50} concentrations for P388-S with 6 nM vinblastine, 10 nM vinorelbine or 110 nM vinflunine. G2/M arrest was assessed by PI staining and by flow cytometry. Comparison of all three vinca alkaloids is shown for P388-S (**a**), P388-N.63 (**b**) and P388-N2.5 (**c**). Data are plotted as the percentage of live cells vs treatment time for vinblastine (*square*), vinorelbine (*circle*) and vinflunine (*triangle*). The data represent the means of two independent experiments with different preps. The error bars represent the standard deviations

24 h and less than 3.0+1.5% after 48 h. At 16 and 24 h for all cell lines the fraction of live cells showed the following pattern vinorelbine > vinblastine > vinflunine.

We also analyzed the extent of mitochondrial membrane depolarization by vinblastine and vinflunine at 10X P388-S IC_{50} concentrations by JC-1 dye using flow cytometry. There was no mitochondrial depolarization at 2, 3, 4 or 8 h by these drugs (Fig. 7). However, differential drug effects on mitochondrial membrane depolarization occurred at 16 and 24 h and were consistent with our G2/M studies: vinflunine > vinblastine > vinorelbine. We evaluated the levels of cytochrome *c* in the cytoplasm upon treatment with vinorelbine, vinblastine and vinflunine after 0 and 16 h. Consistent with the mitochondrial membrane depolarization, we found cytochrome *c* release at 16 h after initiation of drug treatment compared to the no treatment control (data not shown). These results agreed with the more quantitative FACS analysis. The highest amount of cytochrome *c* release occurred in response to vinflunine and vinblastine compared to vinorelbine.

Discussion

Mechanisms of vinorelbine resistance

IC_{50} studies revealed that vinorelbine-resistant cells (P388-N.63 and P388-N2.5) were highly resistant to vinorelbine and also P388-N2.5 were cross resistant to vinblastine; however, both P388-N.63 and P388-N2.5 were relatively sensitive to vinflunine. ATP-Binding-Cassette (ABC) transporters are known to be important efflux pumps in

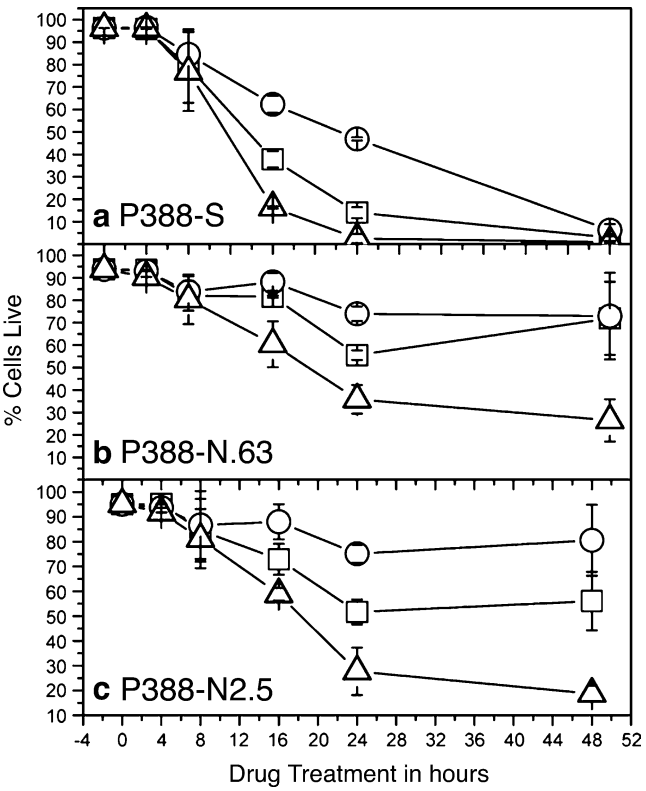

Fig. 6 Apoptosis by vinca alkaloids on P388 vinorelbine-sensitive and -resistant cell lines by flow cytometry. Cells were treated with at 10X IC_{50} concentrations for P388-S with 6 nM vinblastine, 10 nM vinorelbine or 110 nM vinflunine. Early apoptosis (reversal of phosphatidyl serine on plasma membrane) was assessed by dual labeling of cells with Annexin-FITC and PI followed by flow cytometry. Both PI and Annexin-FITC negative populations of cells were gated as live cells and the percentage was plotted against drug treatment in hours. A comparison of all three vinca alkaloids is shown for P388-S (**a**), P388-N.63 (**b**) and P388-N2.5 (**c**) for vinblastine (*square*), vinorelbine (*circle*) and vinflunine (*triangle*). The data are the means of two independent experiments with different cell preps. The error bars represent the standard deviations

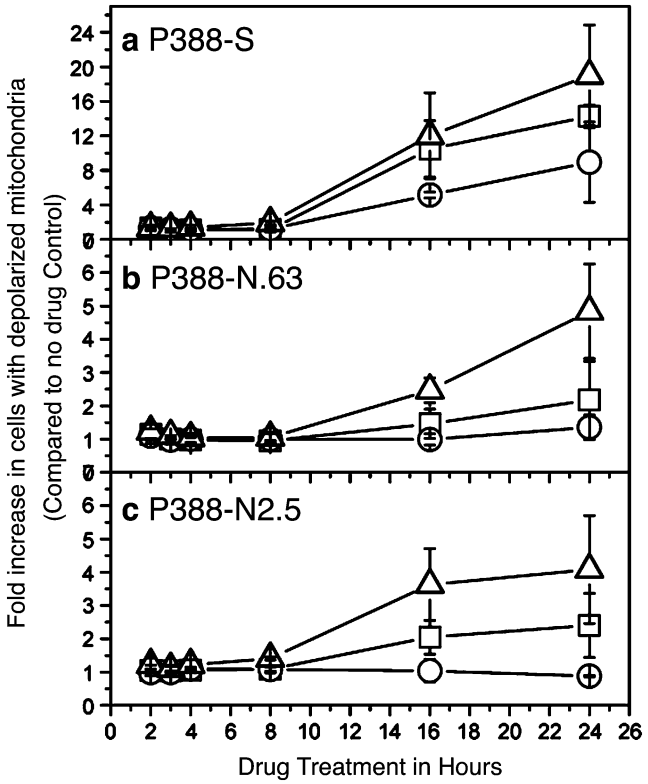

Fig. 7 Mitochondrial membrane depolarization by flow cytometry. Mitochondrial membrane depolarization was assessed by the fluorescence change of JC-1 dye from red to green on transition of the charged mitochondrial membranes to the depolarized state. The *Y*-axis shows the fold-increase in the number of cells containing depolarized mitochondria compared to no drug control. The *X*-axis shows the hours of treatment. Cells were treated with at 10X IC_{50} concentrations for P388-S with 6 nM vinblastine, 10 nM vinorelbine or 110 nM vinflunine. A comparison of all three vinca alkaloids is shown for P388-S (**a**), P388-N.63 (**b**) and P388-N2.5 (**c**) for vinblastine (*square*), vinorelbine (*circle*) and vinflunine (*triangle*). The data represent means of 2–4 experiment for each time point and the error bars represent propagated standard deviations

extruding toxins from cells. Some studies suggest that the ABC transporters, MDR1 and MRP1, are important in the development of drug resistance and are implicated in cell culture resistance to vinca alkaloids. Etievant et al. [8] showed that Pgp-MDR expressing human leukemia, breast and bladder cancer cell lines were the least resistant to vinflunine when compared to vinblastine, vincristine or vinorelbine and consistent with this work, we found that vinorelbine-resistant cell lines expressing Pgp retained sensitivity to vinflunine.

In other work, Ngan et al. [28] suggested that the increased sensitivity of HeLa cells to vinflunine could be explained by the significantly higher intracellular concentration of vinflunine compared to vinorelbine. They suggest that intracellular concentrations of vinblastine and vinorelbine can fall significantly due to the activity of Pgp compared to vinflunine. However this does not explain the relative sensitivity of the vinorelbine-resistant leukemia cells described here to vinblastine, where the IC_{50} value for vinblastine is smaller than for vinorelbine. Thus there must be other explanations for the differential sensitivity of these cells to vinca alkaloids.

Since vinca alkaloids target the interdimer interface and β-tubulin as their receptor [11], we measured possible tubulin changes in these cell lines which might contribute to vinca alkaloid resistance. We did not find any alterations in β-tubulin isotype levels, total tubulin content or microtubule fractions in vinorelbine-resistant cell lines when compared to the drug-sensitive cell line. This suggests it is likely that antimitotic resistance in these cells occurs without alterations in tubulin properties.

In order to investigate the differential sensitivity to vinca alkaloids, we focused on pathways associated with antimitotic-induced G2/M arrest. We first measured the induction of G2/M arrest, apoptosis and mitochondrial membrane depolarization by vinorelbine. There was no significant G2/M arrest when P388 vinorelbine-sensitive and -resistant cells were exposed to IC_{50} concentrations of vinblastine, vinorelbine and vinflunine (data not shown). However at 10X IC_{50}, P388-S cells showed G2/M arrest at 4 h after vinorelbine treatment. After 4 h, the hypodiploid/apoptotic fraction increased. This observation was consistent in four different preps of P388-S and with two different vinorelbine sources. On the other hand in the resistant cell lines, the G2/M or hypodiploid/apoptotic peaks did not appear with vinorelbine treatment even at 10X P388-S IC_{50} concentrations. In the Annexin V/PI studies of apoptosis, P388-S cells became apoptotic at 16 h after initiation of vinorelbine treatment, (8 h after the appearance of G2/M arrest) and less than 10% survived after 48 h of drug treatment. However, in resistant cells 70–80% cells were alive after 48 h of vinorelbine treatment. This suggests that G2/M arrest leads to apoptosis in P388-S cells and that the failure of vinorelbine to cause G2/M arrest in resistant cells leads to enhanced cell survival. In support of the observation that

Table 2 Summary of drug effects on P388 vinorelbine-sensitive and -resistant cell lines

Phenotype	Observed at (hours)	Drug Effect at 10X IC_{50}
G2/M Arrest	4, 8	Vinflunine > vinblastine > vinorelbine
Mitochondrial membrane depolarization	16, 24	Vinflunine > vinblastine > vinorelbine
Apoptosis	16, 24, 48	Vinflunine > vinblastine > vinorelbine
Cytochrome *c* release	16	Vinflunine > vinblastine > vinorelbine

apoptosis occurs via a mitochondrial mediated pathway, the mitochondrial membrane depolarization assay showed that the mitochondria of the P388-S cells were depolarized at 16 h which was 8 h after the appearance of G2/M arrest. No significant mitochondrial membrane depolarization was observed in the vinorelbine-resistant cell lines. Furthermore, no mitochondrial membrane depolarization was found between 2 and 8 h of treatment, suggesting that vinorelbine did not directly affect the mitochondria.

Vinorelbine-resistant cells retain sensitivity to vinflunine

Vinblastine and vinflunine caused G2/M arrest in the P388-S cell line. In addition, vinorelbine-resistant cells also retained sensitivity to vinflunine and to a lesser degree to vinblastine (Table 2). When P388-N.63 and P388-N2.5 were treated with vinblastine or vinflunine, significant G2/M arrest occurred at 8 h and a sub G1 hypodiploid/apoptotic peak appeared at 16 h. It appears that the enhanced ability of vinblastine and vinflunine to cause G2/M arrest in P388 vinorelbine-resistant cells is responsible for the enhanced sensitivity to these drugs. The fold-resistance of the vinorelbine-resistant cells to vinca alkaloids was vinflunine < vinblastine < vinorelbine which is consistent with the extent of G2/M arrest caused by these drugs: vinflunine > vinblastine > vinorelbine (Table 2).

To confirm that G2/M arrest induced by vinca alkaloids leads to apoptosis, we performed time course measurements on the percentage of live cells by AnnexinV-FITC/PI dual labeling flow cytometry. These experiments showed that (1) all three vinca alkaloids were able to kill more than 90% of the P388 vinorelbine-sensitive cells after 48 h via apoptosis; (2) Apoptosis is initiated in vinorelbine-resistant cells after 16 h of vinflunine or vinblastine treatment, (8 h after the appearance of G2/M arrest) and (3) vinflunine caused the most prominent apoptosis in vinorelbine-resistant cell lines beginning at 16 h; whereas vinblastine had a moderate apoptotic effect on resistant cells.

In order to assess the effects of vinca alkaloids on mitochondria-mediated apoptosis at high dose (10X IC_{50}), we measured changes in mitochondrial membrane potential and cytochrome *c* release, major events in mitochondria-mediated apoptosis. We attempted to measure changes in mitochondrial membrane potential at time points as early as 2 h after initiating drug treatment to see if the mitochondria were affected before G2/M arrest. However no changes in the mitochondrial membrane potential were found at 2, 3, 4 and 8 h after drug treatment. We found significant changes in mitochondrial membrane potential in response to vinflunine and vinblastine at 16 and 24 h in all cell lines. We conclude that these drugs do not directly alter the mitochondrial membrane potential. Their effects are found only after the onset of G2/M arrest. Again, vinflunine caused the greatest collapse in mitochondrial membrane potential followed by vinblastine and then vinorelbine. These results indicate that mitochondrial apoptotic pathways are activated following G2/M arrest (4–8 h) in vinorelbine-sensitive and -resistant P388 cell lines. In order of effectiveness at 10X IC_{50} concentrations: vinflunine > vinblastine > vinorelbine (Table 2).

The relationship between vinca alkaloid-induced G2/M arrest and apoptosis warrants further investigation. During mitotic metaphase, spindle fibers pull chromosomes to opposite poles after attaching to kinetochores and cell division proceeds to anaphase. However, vinca alkaloids disturb this process because of insufficient microtubule-kinetochore tension. Mitotic checkpoint proteins like Bub1 detect this defect and signal apoptosis [34] probably through a mitochondria-mediated pathway [25]. Thus we are currently exploring potential differential effects of vinca alkaloids on mitotic checkpoint proteins.

Our studies show that the mitochondria-mediated apoptotic pathway is the major contributor to cell death after G2/M arrest in the murine leukemia cell lines. We showed that vinflunine may have improved activity in certain cancers relative to other vinca alkaloids because of its ability to induce mitochondria-mediated apoptotic pathways through G2/M arrest. There is no evidence that this is due to direct effect on mitochondria or high intracellular drug concentrations. We conclude that multiple resistance mechanisms contribute to drug resistance and that combination therapies directed at one or more of these could boost the effect of antimitotic drugs in cancer treatment and improve patient outcomes.

References

1. Bhattacharya R, Cabral F (2004) A ubiquitous beta-tubulin disrupts microtubule assembly and inhibits cell proliferation. Mol Biol Cell 15:3123–3131
2. Blade K, Menick DR, Cabral F (1999) Overexpression of class I, II or IVb beta-tubulin isotypes in CHO cells is insufficient to confer resistance to Paclitaxel. J Cell Sci 112(13):2213–2221
3. Borst P, Elferink RO (2002) Mammalian ABC transporters in health and disease. Annu Rev Biochem 71:537–592
4. Bosch I, Croop J (1996) P-Glycoprotein multidrug resistance and cancer. Biochim Biophys Acta 1288:F37–F54
5. Caceres A, Binder LI, Payne MR, Bender P, Rebhun L, Steward O (1984) Differential subcellular localization of tubulin and the microtubule-associated protein MAP2 in brain tissue as revealed by immunocytochemistry with monoclonal hybridoma antibodies. J Neurosci 4:394–410
6. Cossarizza A, Baccarani-Contri M, Kalashnikova G, Franceschi C (1993) A new method for the cytofluorimetric analysis of mitochondrial membrane potential using the J-aggregate forming lipophilic cation 5,5′6,6′-tetrachloro-1,1′,3,3′-tetraethylbenzimidazolcarbocyanine iodide (JC-1). Biochem Biophys Res Commun 197:40–45

7. Dumontet C, Jaffrezou JP, Tsuchiya E, Duran GE, Chen G, Derry WB, Wilson L, Jordan MA, Sikic BI (2004) Resistance to microtubule-targeted cytotoxins in a K562 leukemia cell variant associated with altered tubulin expression and polymerization. Bull Cancer 91:E81–E112
8. Etievant C, Barret JM, Kruczynski A, Perrin D, Hill BT (1998) Vinflunine (20′,20′-difluoro-3′,4′-dihydrovinorelbine), a novel vinca alkaloid, which participates in P-glycoprotein (Pgp)-mediated multidrug resistance in vivo and in vitro. Invest New Drugs 16: 3–17
9. Etievant C, Kruczynski A, Barret JM, Tait AS, Kavallaris M, Hill BT (2001) Markedly diminished drug resistance-inducing properties of vinflunine (20′,20′-difluoro-3′,4′-dihydrovinorelbine) relative to vinorelbine, identified in murine and human tumour cells in vivo and in vitro. Cancer Chemother Pharmacol 48:62–70
10. Fabbri F, Carloni S, Brigliadori G, Zoli W, Lapalombella R, Marini M (2006) Sequential events of apoptosis involving docetaxel, a microtubule-interfering agent: a cytometric study. BMC Cell Biol 7:6
11. Gigant B, Wang C, Ravelli RB, Roussi F, Steinmetz MO, Curmi PA, Sobel A, Knossow M (2005) Structural basis for the regulation of tubulin by vinblastine. Nature 435:519–522
12. Hari M, Yang H, Zeng C, Canizales M, Cabral F (2003) Expression of class III beta-tubulin reduces microtubule assembly and confers resistance to paclitaxel. Cell Motil Cytoskelet 56: 45–56
13. Hill BT (2001) Vinflunine, a second generation novel vinca alkaloid with a distinctive pharmacological profile, now in clinical development and prospects for future mitotic blockers. Curr Pharm Des 7:1199–1212
14. Hiser L, Aggarwal A, Young R, Frankfurter A, Spano A, Correia JJ, Lobert S (2006) Comparison of beta-tubulin MRNA and protein levels in 12 human cancer cell lines. Cell Motil Cytoskelet 63:41–52
15. Jacquesy J, Fahy J (2000) Cancer: superacid generation of new antitumor agents. In: Torrence PF (ed) Biomedical chemistry: applying chemical principles to the understanding and treatment of disease. Wiley, New York, pp 227–245
16. Kruczynski A, Barret JM, Etievant C, Colpaert F, Fahy J, Hill BT (1998) Antimitotic and tubulin-interacting properties of vinflunine, a novel fluorinated vinca alkaloid. Biochem Pharmacol 55: 635–648
17. Kruczynski A, Hill BT (2001) Vinflunine, the latest vinca alkaloid in clinical development. A review of its preclinical anticancer properties. Crit Rev Oncol Hematol 40:159–173
18. Kruczynski A, Etievant C, Perrin D, Chansard N, Duflos A, Hill BT (2002) Characterization of cell death induced by vinflunine, the most recent vinca alkaloid in clinical development. Br J Cancer 86:143–150
19. Lee MK, Tuttle JB, Rebhun LI, Cleveland DW, Frankfurter A (1990) The expression and posttranslational modification of a neuron-specific beta-tubulin isotype during chick embryogenesis. Cell Motil Cytoskelet 17:118–132
20. Lobert S, Correia JJ (2000) Energetics of vinca alkaloid interactions with tubulin. Methods Enzymol 323:77–103
21. Lobert S, Frankfurter A, Correia JJ (1995) Binding of vinblastine to phosphocellulose-purified and alpha beta-class III tubulin: the role of nucleotides and beta-tubulin isotypes. Biochemistry 34:8050–8060
22. Lobert S, Frankfurter A, Correia JJ (1998) Energetics of vinca alkaloid interactions with tubulin isotypes: implications for drug efficacy and toxicity. Cell Motil Cytoskelet 39:107–121
23. Lobert S, Ingram JW, Hill BT, Correia JJ (1998) A Comparison of thermodynamic parameters for vinorelbine- and vinflunine--induced tubulin self-association by sedimentation velocity. Mol Pharmacol 53:908–915
24. Lobert S, Fahy J, Hill BT, Duflos A, Etievant C, Correia JJ (2000) Vinca alkaloid-induced tubulin spiral formation correlates with cytotoxicity in the leukemic L1210 cell line. Biochemistry 39: 12053–12062
25. Masuda A, Maeno K, Nakagawa T, Saito H, Takahashi T (2003) Association between mitotic spindle checkpoint impairment and susceptibility to the induction of apoptosis by anti-microtubule agents in human lung cancers. Am J Pathol 163:1109–1116
26. Minderman H, Vanhoefer U, Toth K, Yin MB, Minderman MD, Wrzosek C, Slovak ML, Rustum YM (1996) DiOC2(3) is not a substrate for multidrug resistance protein (MRP)-mediated drug efflux. Cytometry 25:14–20
27. Minotti AM, Barlow SB, Cabral F (1991) Resistance to antimitotic drugs in Chinese hamster ovary cells correlates with changes in the level of polymerized tubulin. J Biol Chem 266: 3987–3994
28. Ngan VK, Bellman K, Hill BT, Wilson L, Jordan MA (2001) Mechanism of mitotic block and inhibition of cell proliferation by the semisynthetic vinca alkaloids vinorelbine and its newer derivative vinflunine. Mol Pharmacol 60:225–232
29. Noble RL (1990) The discovery of the vinca alkaloids-chemotherapeutic agents against cancer. Biochem Cell Biol 68:1344–1351
30. Pourroy B, Carre M, Honore S, Bourgarel-Rey V, Kruczynski A, Briand C, Braguer D (2004) Low concentrations of vinflunine induce apoptosis in human SK-N-SH neuroblastoma cells through a postmitotic G1 arrest and a mitochondrial pathway. Mol Pharmacol 66:580–591
31. Roach MC, Boucher VL, Walss C, Ravdin PM, Luduena RF (1998) Preparation of a monoclonal antibody specific for the class I isotype of beta-tubulin: the beta isotypes of tubulin differ in their cellular distributions within human tissues. Cell Motil Cytoskelet 39:273–285
32. Scarlett JL, Sheard PW, Hughes G, Ledgerwood EC, Ku HH, Murphy MP (2000) Changes in mitochondrial membrane potential during staurosporine-induced apoptosis in Jurkat cells. FEBS Lett 475:267–272
33. Sullivan KF, Cleveland DW (1986) Identification of conserved isotype-defining variable region sequences for four vertebrate beta tubulin polypeptide classes. Proc Natl Acad Sci USA 83:4327–4331
34. Taylor SS, McKeon F (1997) Kinetochore localization of murine Bub1 is required for normal mitotic timing and checkpoint response to spindle damage. Cell 89:727–735
35. Wang Y, Cabral F (2005) Paclitaxel resistance in cells with reduced beta-tubulin. Biochim Biophys Acta 1744:245–255